# Development of a Compact Imaging Spectrometer Using Liquid Crystal Tunable Filter Technology

*Jessica A. Faust, Abhijit Biswas, Gregory H. Bearman, Thomas Chrien,*
*NASA Jet Propulsion Laboratory*

*Peter J. Miller*
*Cambridge Research & Instrumentation, Inc.*

## Abstract

1 .iquid crystal tunable filters arc useful in building compact multi-spectral instruments. The system is portable and adaptable for use in a variety of folds of stud y in the visible and near-infrared regions Or the spectrum. We will present data from cal ibration targets and some applications, results of the spectral calibration of a spectrometer system, and results of environmental (vibration, radiation, shock, and thermal) testing. Data acquisition and system design arc also discussed.

## System Characteristics

The compact imaging spectrometer uses a liquid crystal tunable filter (1 .CTF) for wavelength selection in image capture. A CCD came.ra looks through a 1 .CTF at an i lluminated object of interest and captures data cube.s by selecting a wavelength and taking an image repeatedl y until an entir c data cube is formed. Images and header information are saved in band sequential (BSQ) for m.

Components of the system are a scientific grade silicon CCD array; a telephoto lens mounted to the camera; and a Liquid Crystal "J'unable filter. Presently in use is 1 6-bit camera with 1024X 1 ()?.4 pixels for the region out to 1.1 µm and a thermal imaging camera with 256x256 pixels for the region from 1.1 -?.4 pm. A 12-bit silicon CCD army of 1 536x1024 pixels has also b een used Successfully. The telephoto lens be ing used with the CCD is dependent upon the application.

1 .CTF's arc continuously [unable. over a given spectral range, have millisecond tuning speeds, and can be tuned randomly. Current filters cover 400-7? ()" nm, (X)( )-1 100"11111, and 1.1-2.411111. A typical visible filter has a nominal 10 nm bandpass and can be tuned in steps as small as ().1 nm. The 1 .CTF passband increases with wave.lcllgth, for a nominal 1() nm bandpass:
Equation 1:

$$\sigma(\lambda) \approx 5 * \left(\lambda / 400\text{nm}\right)^2,$$

therefore the spectral bandwidth of a filter can range from 5-16 nm. Transmission also varies as a function of wave.lcrlg[iI, extending from approximately 5% in the blue region up to nearly 60% at 700" nm for the visible filters. 1 .CTF's arc low mass and power and are suitable for planetary missions.

## Environmental Testing of the LCTF

A complete set of environmental tests was per formed on the liquid crystal tunable filters. In the vibration tests, the filter received, without damage, up to 30 g on 3 axes (above Cassini and Rosetta *instrument* levels) and shock tests up to 200 g at a maximum of 3000 117. (Cassini and Champollion *instrument* levels).

1 .iquid crystal tunable filters consist of polarizers, glasses, epox its, and liqu id crystals. Out-gassing of the com]mlIc.ills can damage other instrument optics. Several of the components were found in the NASA Thermal/Vacuum 1 Database, two others were tested. Both passed the standing JPL requirements for thermal/vac uum performance.

A working filter underwent repeated thermal cycling from -30°C to room temperature over the duration of one year and continued to function. A filter also underwent thermal cycling from room temperature to 150 Kelvin without delamination of the stages or 10ss of functionality of the filters.

Five liquid crystal cells and three polarizers underwent a radiation test with a cobalt-60 γ source at 5/1 ()/1 5/?[])/1 000" Krads. A dose rate of 1rad per second allowed for some self-annealing in the cells. Optical and electro-optical properties of al I the male.rids were measured after each radiation exposure, including the transmission of the bulk retarders and polymers, polarizer extinction, and transmission and electro-optical tuning (retardance versus applied voltage) of the liquid crystal cells. Any changes in tuning with radiation will show up as shifts in the passband wavelength and increases in out-of-band transmission.

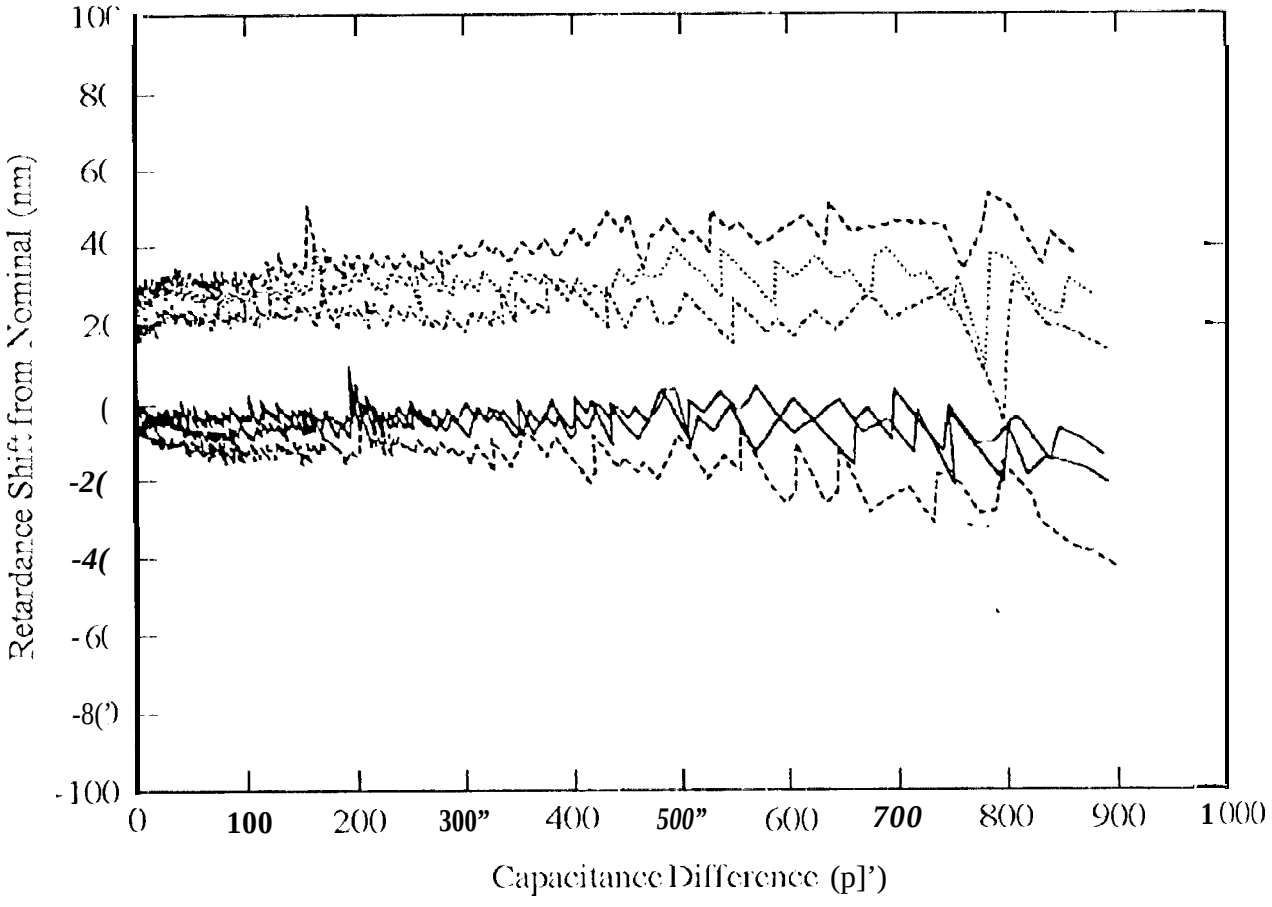


Figure 1. Retardance Shift of Liquid Crystal cell F for changes in capacitance with drive voltage.

Since the tuning of the device is accomplished electro-optically, that parameter must also be examined. There is a shift in the, tuning at any wavelength of a single stage of the LCTF given by $\Delta = 2 * d\lambda * \phi/\lambda_o$. ***41*** is the retardance parameter calculated from the radiation dab. The maximum value. for $\phi$ is -lo nm, llmrc.fore, at 800" nm with a $d\lambda$ of 10 nm the tuning shift is only 1 nm (lo% of the FWHM).

What is important here is that the shift is well within the self-c:]lil~t:iti(~l] range Of an LCTF filter. The filter can return its wavelength calibration with a single fixed wave.lc.rIgllI from a laser diode. In fact, that is how the tuning curve for each filter is determined at the factory; those tuning curves are then burned into firmware for the

controller. A flight instrument would naturally have such a calibration capability anyway.

Darkening was the major effect was for all the optical components (including the sheet polarizers). A loss of less than 15% at 20 Krad was seen for the visible polarizers. Quartz samples also showed a ~0.5% ± 0.5% transmission loss. Changing the filler to a Sole design instead of the present 1-yot design used would decrease the number of polarizers in the system, reducing radiation effects and increasing system transmission.

## Spectral Calibration

Wavelength accuracy and bandwidth were measured a helium-moll laser. First, the spectrometer function was measured in order to properly calibrate the He-Ne image cube. A calibrated NIST standard 1000 Watt bulb uniformly illuminates a 10 inch spectralon panel through a circular baffle at a distance of 50 cm; the camera spectrometer is set-up at an angle to the panel. This was used to determine the response of the spectrometer system. Equation 2:

$$\text{Response} = \frac{\text{average}(DN_{pixel})}{\text{normalized}(E_{1000W} * R_{panel})}$$

Using the calculated source characteristics (derived from the known panel reflectance and known bulb irradiance) allows the spectrometer response to be derived directly from the image cube. Next, a He-Ne laser illuminates the panel, a simple lens expands the beam, and a diffuser makes the illumination uniform across the panel. An image cube is captured over the range of 600-660 nm at 2 nm steps (the filter used has approximately a 10 nm bandpass). Spectrometer response, calculated earlier, is interpolated and normalized over the wavelength range of interest for use with the image cube data. Each slice of the image cube is averaged and calculations done on both averages and individual pixels. Data from the He-Ne laser is corrected by dividing out the panel response and a simple gaussian fit determines the peak and width of the laser beam source. As seen in figure 2, the spectrometer data has the peak at 632.37 nm with a full width half maximum of 12.67 nm. The shift from the peak is 0.43 nm, well below the filter reproducibility of $\Delta\lambda = \sigma/8$ ($\Delta\lambda = 12.67\text{ nm} / 8 = 1.58$ nm).

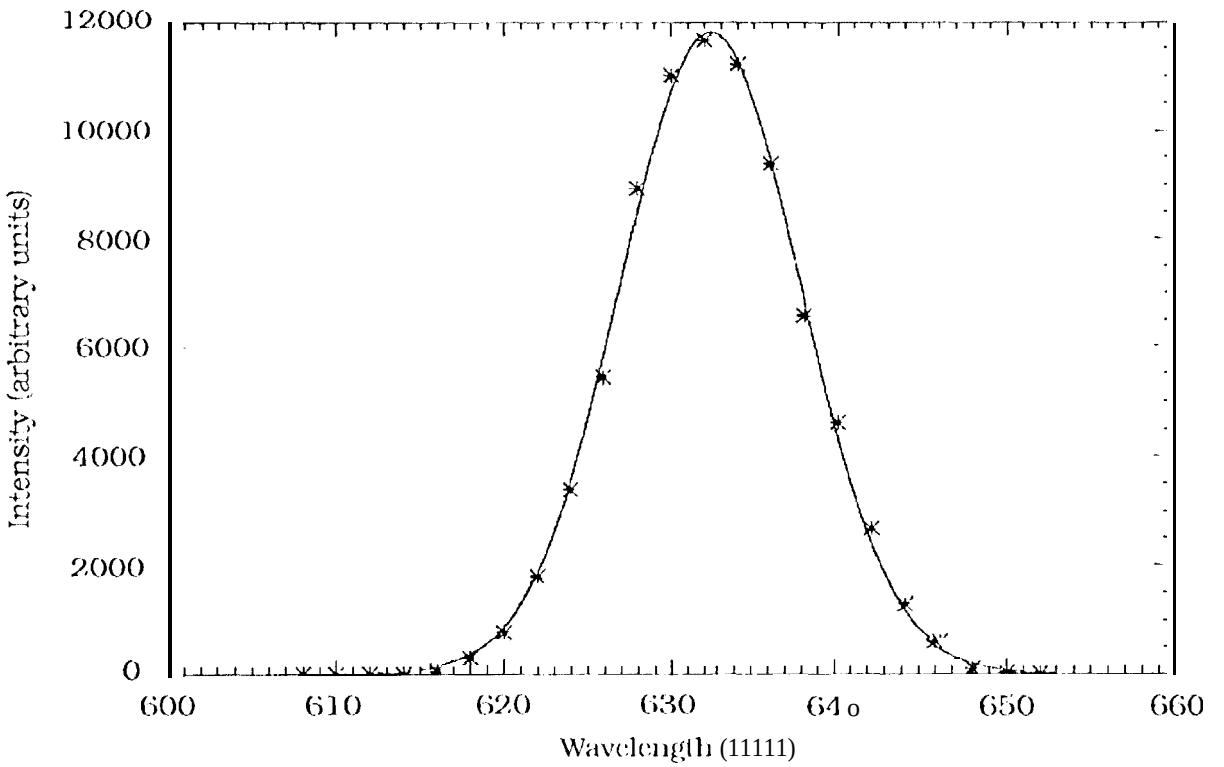


Figure 2. Intensity Profile of a He-Ne laser compared with spectrometer results

A similar experiment was done with the spectrometer focused on the exit slit of a monochromator using various slit widths and wavelengths. Wavelength calibrations using the monochromator behave similarly as shown with the laser line. As expected, the slit width does not have, an affect 011 the full width half maximum or the peak wavelength.

Labsphere color targets and a 99% reflectance target (Labsphere Spectralon) are used to compare the camera spectrometer data directly with 1 .absphere's calibration. Spectralon targets are used as reference and are used to correct the color target images. Reflectances are talc.ulakxi as shown below:

Equation 3:

$$\text{Reflectance}(\lambda) = \frac{(DN_{color}/\tau_{target} - \text{bias} - \text{dark})}{(DN_{ref}/\tau_{ref} - \text{bias} - \text{dark})}$$

$\tau$: Integration time for eacl I image. slice

Figures 3A-D illustrate reflectance rc.suits of this method. Figures 3A and 3B are for the blue color target and figures 3C and 3D are for the red color target. The results of this talc.ulal ion arc. compared with the 1 .absphere target calibration data in all figure.

Visible LCTFs (400-720" nm) begin to transmit at -740 nm as the polarizers begin to fail. In figure.s 3A and 3C, a custom hot mirror is added used but it also turns back on near 100011111. Evidence of the leakage problem is seen in the overcounting of photons across the entire wavelength range. In order to prevent the "blue blow up" and the overcounting in the red regi on, using a proper filter is a necessity. In figures 3B and 3D, the hot mirror was paired with a Schott 11(;18 glass filter. The hot mirror and filler glass combine well with the filter to take away the problem of overcounting of photons and leave the instrument under-reporting the targets by a few percent.

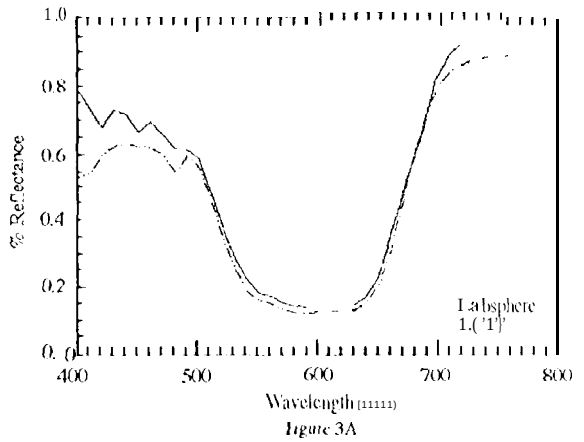

Figure 3A

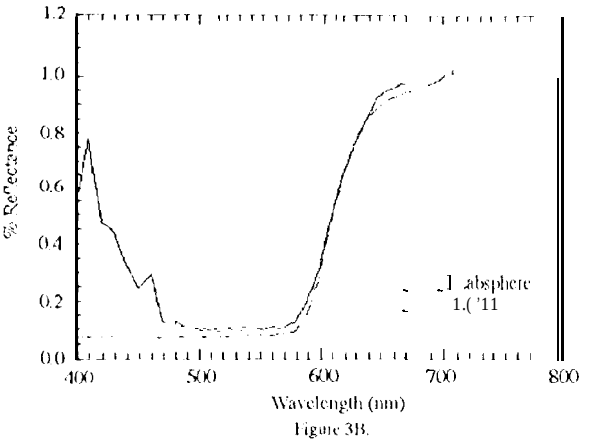

Figure 3B.

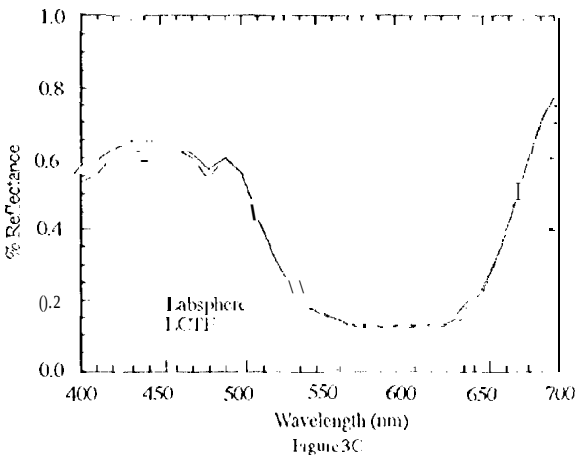

Figure 3C

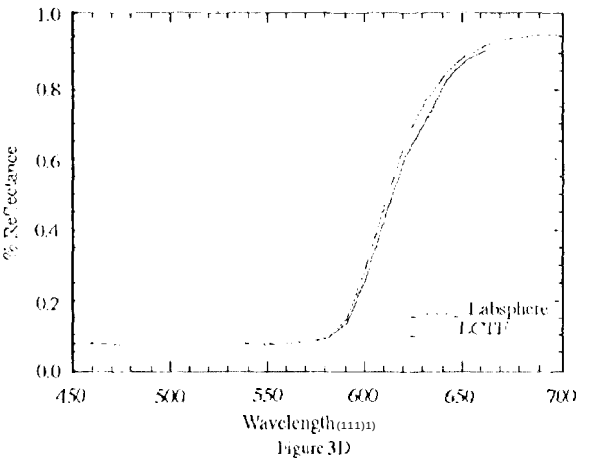

Figure 3D

Figure 3A-D. Data taken using Labsphere color targets compared with Labsphere calibration data.

## Data Acquisition and System Design

We currently have a data acquisition system in the advanced development stages. Visual C++, running in Windows on a PC, is being used to design and implement an interface for the user's. An illumination calculation program in IDL determines the exposure times using a small image cube taken with the acquisition routine and writes out a header file,. JPLImage (oar Visual C++ program) reads the header file written by the IDL illumination program and uses it to capture the data cube. JPLImage works with our ().4 -().7 mm and 0.6- 1.1 mm filters and several cameras. It allows for dire.cl control of the filters and cameras. Data collection results in individual image frames or image cubes. Dark and bias imaging modes and a focus modem also available to the user.

Future development of the acquisition program is underway. Steps described above for using an 11)1. routine to calculate the illumination curve, will be integrated into the JPLImage program in order to make the data capture autonomous. The final evolution of JPLImage will be to turn it into flight software that will control the spectrometer system on the Rocky 7 Mars Rove.r.

## Advantages and Uses of the System

Compact spectrometers arc useful in many different fields of study because the system is easily transportable and can be used in applications that require. imaging nearby or al a reasonable distance. The system is in use. in plant physiology, neurological imaging, archaelogy, and geology experiments.

Other applications for the system exist in bio-medical imaging including tumors, dysplasias, detected through spectrum, oximetry and blood flow, what biologically active molecules arc wher c., and more. Agricultural uses are also abundant, including water stress in plants-irrigation scheduling, plant health - is photosynthesis occurring, crop identification, harvesting, and monitoring plant disease and application of pesticides and herbicides.

LCTF spectrometers are low power and mass making it particularly useful for space-based applications. Liquid crystal tunable fillers can be built for specific applications by choosing the bandpass carefully, allowing scientists to lower the cost, sire, and mass. The bandpass can be made as wide or as narrow as needed. Not all applications need a 16-bit camera, so different cameras can also be chosen for specific tasks.

A prototype instrument is being designed and built for the Rocky 7 Mars Rover demonstration project. A 10-bit CUSTOM APS (active pixel sensor) camera coupled with a compact lens (optimized for the LCTF) will be used for image capture. Repackaging of a visible. LCTF will reduce the size and mass Or the instrument which will have a total mass of approximately 800 grams. Total power required for the instrument is 1-2 Watts. The filter itself draws no power while the LCTF tuning voltages are less than 20 Volts; the only power load comes from the control electronics.

## Examples of Applications and Results

The first use of the camera spectrometer was imaging of the Dead Sea Scrolls (DSS). Many of the DSS have faded over lime. and are illegible. Image cubes of several fragments explained why infrared photography yields more legible images than visible photography.[1] In addition, we developed a simple system for imaging at 9-/0 nm (much further in the NIR than film) that provides realtime images ready for the text scholar. Images from a 1994 field expedition to Jerusalem have been used as the basis for a new transcription and reconstruction of an important DSS, the Genesis Apochryphon.

Detecting, monitoring, and staging of periodontal disease is being studied with the spectrometer. Current staging of gingivitis is relatively crude and subject to each individual doctor's opinion. The focus of the study is to determine quantitatively the stages of gingval disease. This includes being able to detect and monitor the gingivae throughout the treatment process.

A method of determining the thickness of ice on aircraft surfaces is being developed.[2] Spectal reflectance varies with the depth of ice and/or water on a known aircraft surface material (typically, aluminum). This is accomplished by looking at the water and ice absorption bands between 900-"1100 nm. With the use of an imager (such as the LCTF spectrometer), the thickness of ice over an area can be mapped out. Also, ice can be differentiated from waler because its spectral reflectance is different from that of water.

An experiment in functional brain mapping using the compact spectrometer is ongoing at this time. A functional mapping of the brain can be done using the spectral signature to correlate with known histo-pathology.

In macademia nut harvesting, the system can be used in grading the nuts. Using the spectometer to grade the nuts will simplify the sorting process, allowing quicker production times.

## Future Work

Future work includes the completion of the autonomous data acquisition system; the repackaging of the filters into the small, low mass package to be used on the Mars rover; and the demonstration of the technology on Rocky '1.

## References

1. Bearman, G. and Spiro, S.I. "Archelogical Applications of Advanced Imaging Techniques". Biblical Archeologist 59: 56-66 (1996).
2. Bearman, G et al. "Optical Remote Detection of Ice on Aircraft Surfaces". NASA Tech Brief NPO-19929. June, 1996.